Magn Reson Med Sci 2021; 20; 175–181
doi:10.2463/mrms.mp.2020-0016
Published Online: July 9, 2020

MAJOR PAPER

Distribution of Gadolinium-based Contrast Agent after Leaking into the Cerebrospinal Fluid: Comparison between the Cerebral Cisterns and the Lateral Ventricles

Toshio Ohashi[1*], Shinji Naganawa[2], Saeko Iwata[1], and Kayao Kuno[3]

Purpose: Leakage of a small amount of intravenously administered gadolinium-based contrast agents (GBCAs) into the cerebrospinal fluid (CSF) space has been reported, even in healthy subjects without blood–brain barrier disruption. Several candidates including the choroid plexus and cortical veins have been proposed as the source of the leakage. The purpose of this study was to evaluate the distribution of intravenously administered GBCA leakage into the CSF by comparing the contrast enhancement of the cerebral cisterns to the lateral ventricles (LVs).

Methods: In 26 patients with a suspicion of endolymphatic hydrops (21–80 years old), a three-dimensional real inversion recovery (3D-real IR) image was obtained at pre-, and at 5 min, and 4 h post-intravenous administration of a single dose of GBCA (IV-SD-GBCA). In the 3D-real IR image, the signal intensities (SIs) in the anterior horn of the LV (LV_{ante}), the trigone of the LV (LV_{tri}), the Sylvian fissure (SyF), the ambient cistern (Amb), the prepontine cistern (PPC), the cerebellopontine angle cistern (CPA), and the vitreous (Vit) were measured. The differences in the SI at pre-, and at 5 min and 4 h post-IV-SD-GBCA were evaluated for each region. The change in the SI pre- to post-IV-SD-GBCA (SI_{change}) were calculated for each region. The differences in the SI_{change} in each region were evaluated at 5 min and 4 h post-IV-SD-GBCA. A Steel-Dwass's test was applied to correct for multiple comparisons.

Results: The SIs of all regions at 4 h post-IV-SD-GBCA were significantly higher compared with pre-IV-SD-GBCA ($P < 0.05$). The SI_{change} in the SyF, Amb, PPC, and the CPA were significantly higher compared with those of the LV_{ante}, LV_{tri}, and the Vit at 4 h post-IV-SD-GBCA ($P < 0.05$).

Conclusion: The contrast enhancement in the cerebral cisterns was greater than that in the LVs.

Keywords: *magnetic resonance imaging, gadolinium, cerebrospinal fluid, gadolinium leakage*

Introduction

It has been thought that gadolinium-based contrast agents (GBCAs), which maintain an intact chelate, do not cross the brain–blood barrier, nor directly enter into the brain parenchyma. However, gadolinium accumulation after repeated intravenous administrations of GBCAs (IV-GBCAs) in the brain parenchyma, such as the dentate nucleus and the globus pallidus, has been demonstrated.[1] Heavily T_2-weighted three-dimensional fluid-attenuated inversion recovery (hT_2W-3D-FLAIR) imaging is highly sensitive to T_1 shortening in fluid compartments, which cannot be detected with conventional T_1-weighted imaging.[2,3] Previously reported studies using hT_2W-3D-FLAIR imaging showed that intravenously administered GBCAs leak into the cerebrospinal fluid (CSF) and perivascular space (PVS) in the basal ganglia of healthy human subjects without renal insufficiency,[4] as well as animals.[5,6] The PVS comprises the glymphatic system, which has been hypothesized as a waste clearance system in the brain.[7] This clearance depends on the CSF–interstitial fluid exchange via the PVS.[7] Therefore, it is presumed that such fluid dynamics might be involved in the penetration of intravenously administered GBCAs into the CSF as well as the brain parenchyma.[8,9] However, the pathway by which GBCAs

[1]Department of Radiology, Kamiiida Daiichi General Hospital, Aichi, Japan
[2]Department of Radiology, Nagoya University Graduate School of Medicine, Aichi, Japan
[3]Department of Otorhinolaryngology, Kamiiida Daiichi General Hospital, Aichi, Japan

[*]Corresponding author: Department of Radiology, Kamiiida Daiichi General Hospital, 2-70, Kamiiida-kitamachi, Kita-ku, Nagoya, Aichi 462-0802, Japan. Phone: +81-52-991-3111, Fax: +81-52-981-6879, E-mail: t.ohashi@re.commufa.jp

Received: January 29, 2020 | Accepted: April 24, 2020

in the blood vessels leak into the CSF is still under discussion. Several candidates, such as the peripheral part of cranial nerve, the circumventricular organs, the choroid plexus, and the cortical veins including vein of Labbe, have been proposed as this leakage route.[10–14]

In our hospital, hT_2W-3D-FLAIR imaging is routinely performed for the evaluation of inner ear endolymphatic hydrops (EH).[15,16] Using signal intensity (SI) measurement of the CSF on hT_2W-3D-FLAIR imaging, we reported that the vein of Labbe was a candidate for the pathway by which intravenously administered GBCAs leak into the CSF space.[14] However, we could not evaluate the lateral ventricle (LV) because the field of view of the hT_2W-3D-FLAIR imaging was limited to the lower half of the brain. Three dimensional-real inversion recovery (3D-real IR) imaging was developed to evaluate EH after IV-GBCA without the requirement for post-processing of multiple imaging series.[17] This imaging method is based on phase-sensitive reconstruction, which allows the visualization of positive and negative longitudinal magnetization separately, and consequently prevent the paradoxical signal loss caused by slight GBCA in fluid appearing in hT_2W-3D-FLAIR imaging based on magnitude reconstruction.[17] The 3D-real IR images can reduce the risk of misregistration artifacts caused by patient motion, and thus, we routinely obtain a 3D-real IR image as a supplementary image in an EH examination.[18] The whole brain is included in the 3D-real IR image, which permits the evaluation of the LV.[18] In these images, we noticed that there was a difference in the contrast enhancement, which represented a difference of GBCA distribution between the ventricles and the cisterns. We speculated that the leakage pathway might be estimated by comparing the contrast enhancement of the CSF in various locations, because more GBCA would be found in CSF adjacent to a leakage site.

The purpose of this study was to retrospectively evaluate the distribution of intravenously administered GBCA leakage into the CSF by comparing the contrast enhancement of the cerebral cisterns to the LVs using 3D-real IR imaging.

Materials and Methods

Patients and materials

The subjects of this study were 26 patients (men: 13, women: 13, ages: 21–80 years old, median: 55.5 years old) with clinically suspected EH who underwent MRI from November, 2017 through April, 2019. The estimated glomerular filtration rate of all patients exceeded 60 mL/min/1.73 m^2. The Medical Ethics Committee of our hospital approved this retrospective study and waived informed consent. All MRI was performed on a 3T MR scanner (MAGNETOM Skyra; Siemens Healthcare, Erlangen, Germany) with a 32-channel phased-array head coil. The contrast agent administered to patients in this study was a macrocyclic GBCA (Gd-HP-DO3A: ProHance; Eisai, Tokyo, Japan). A single dose of GBCA (SD-GBCA) was defined as 0.1 mmol/kg body-weight. The image analyses were performed with a DICOM viewer (OsiriX version 5.8 32 bit; Pixmeo SARL, http://www.osirix-viewer.com/). The statistical analyses were performed with free statistical software (R software version 3.6.1; The R Foundation, https://www.r-project.org/).

Magnetic resonance imaging

The 3D-real IR imaging was based on a hT_2W-3D turbo spin echo sequence with a variable refocusing flip angle (TR = 15,130 ms, TE = 544 ms). For the non-slab selective IR preparation pulse, we set the waiting time to 2700 ms to obtain a negative SI in the endolymph and CSF, which did not contain GBCA. The voxel size was 0.5 × 0.5 × 1.0 mm^3. The slab oblique angle was set parallel to the anterior commissure–posterior commissure line and the bilateral internal auditory canal. The slab thickness was 256 mm, and the center of the imaging slab was placed at the mammillary body. The parameter details are indicated in Table 1. The 3D-real IR imaging was obtained at pre-, and at 5 min and 4 h post-IV-SD-GBCA.

Image analysis

We corrected the misregistration over the time of the acquisition, using an OsiriX function, which was based on manual pixel alignment. In the pre-administration 3D-real IR image, we manually placed circular regions of interest (ROIs) with a diameter of 3.0 mm in the bilateral following region: the anterior horn of the LV (LV_{ante}), the trigone of the LV (LV_{tri}), the Sylvian fissure (SyF), the ambient cistern (Amb),

Table 1 Detailed pulse sequence parameters

Pulse sequence name	3D-real IR
Pulse sequence type	SPACE with inversion pulse
Repetition time (ms)	15130
Echo time (ms)	549
Inversion time (ms)	2700
Fat suppression	CHESS
Flip angle (°)	90/constant 145
Section thickness/gap (mm)	1.0/0.0
Pixel size (mm)	0.5 × 0.5
Number of slices	256
Echo train length	256
Field of view (mm)	165 × 196
Matrix size	324 × 384
Parallel imaging/Accel. factor	GRAPPA/3
Band width (Hz/Px)	434
Number of excitations	1
Scan time (min)	11.4

3D-real IR, 3D real inversion recovery (phase sensitive reconstruction); CHESS, chemical shift selective; GRAPPA, generalized auto-calibrating partially parallel acquisition; SPACE, sampling perfection with application-optimized contrasts using different flip angle evolutions.

the prepontine cistern (PPC), the cerebellopontine angle cistern (CPA), and the vitreous (Vit). An example of the ROI placement is indicated in Fig. 1. These ROIs were copied and pasted onto the images obtained at 5 min and 4 h post-IV-SD-GBCA. We measured the SI in the ROIs and averaged the values for the bilateral region. The change in the SI pre- to post-IV-SD-GBCA (SI_{change}) was calculated. Two radiographers with 16 (T.O.) and 6 years (S.I.) experience in MRI were responsible for the image analyses.

Statistical analysis

The inter-observer reliability was evaluated using an intraclass correlation coefficient (ICC) (2, 1). The averaged value from the two observers was used for the statistical analyses. Significant differences between the SI measured at pre-IV-SD-GBCA and those at 5 min and 4 h post-IV-SD-GBCA were evaluated for each ROI. Significant differences between the SI_{change} in each ROI were evaluated at 5 min and 4 h post-IV-SD-GBCA. A Steel-Dwass's test was applied to correct for multiple comparisons. We defined 5% as a threshold for statistical significance.

Results

The ICCs (2, 1) between the two observers were 0.973 for the SI measurement at pre-IV-SD-GBCA, 0.956 for 5 min post-, and 0.986 for 4 h post-IV-SD-GBCA. No significant differences were found between the SI measured at pre- and 5 min post-IV-SD-GBCA, for any regions. A significant difference was found between the SI at 5 min and 4 h post-IV-SD-GBCA, for all regions. A significant difference was observed between the SI measured at pre- and 4 h post-IV-SD-GBCA, in all regions (Fig. 2). The *P*-values for the multiple comparison of the SI was summarized in Table 2. A significant difference was found between the SI_{change} of Vit and that of the other regions at 5 min post-IV-SD-GBCA. A significant difference was found between the SI_{change} of LV_{ante}, LV_{tri}, and Vit and that of SyF, Amb, PPC, and CPA, at 4 h post-IV-SD-GBCA (Fig. 3). The *P*-values for the multiple comparison of the SI_{change} was summarized in Table 3. Representative images are indicated in Fig. 4.

Discussion

We considered that using the ratio of SI was inappropriate for this evaluation, because the values of SI in the 3D-real IR image based on phase-sensitive reconstruction includes not only positive value but also negative value and brain parenchyma shows near zero signal.[17] Therefore, we used the SI and the SI_{change} in the cisterns, the LVs, and the Vit for the evaluation of the contrast enhancement. The SI was increased in all CSF spaces as well as the Vit at 4 h post-IV-SD-GBCA compared with pre-administration. These findings support previous studies using hT_2W-3D-FLAIR imaging after IV-SD-GBCA.[10,11] In addition, the SI increase in the cisternal CSF was higher than that in the LVs at 4 h post-IV-SD-GBCA. Therefore, the intravenously administered GBCA that had leaked into the CSF was considered to be at a higher concentration in the cisterns than in the LVs. In the previous study on the regular contrast 3D-FLAIR using variable flip angle echo train readout, a flow velocity-related SI decrease of GBCA dissolved fluid was observed.[19] In this present study, any discernable decrease in the SI of the CSF was not

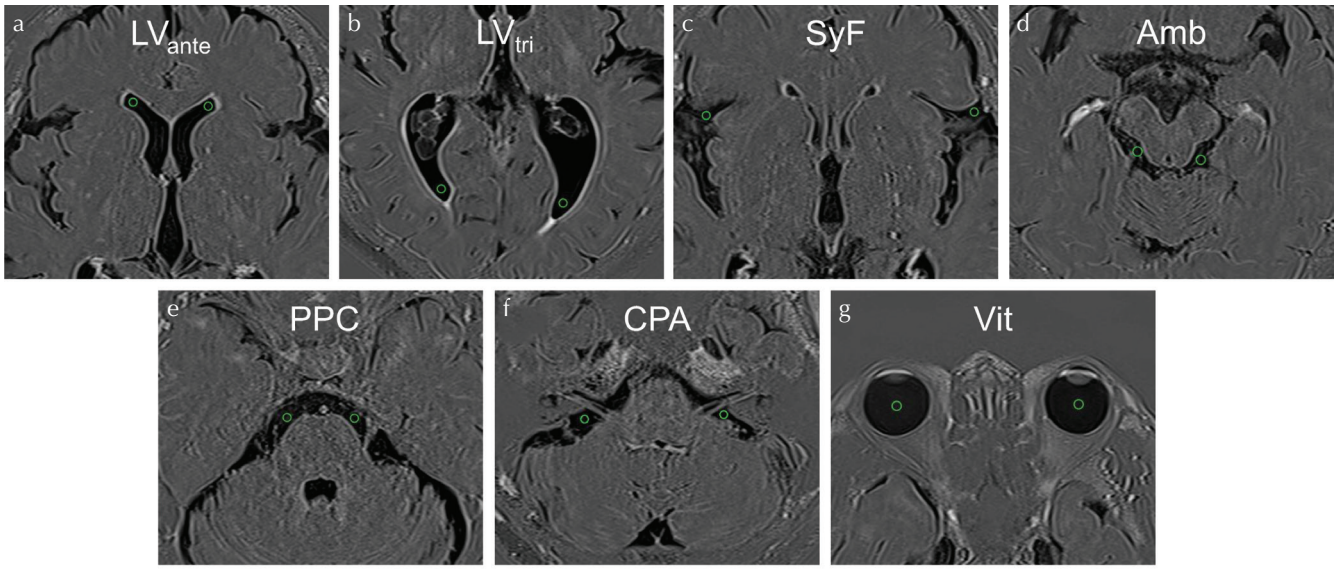

Fig. 1 An example of the ROI placement for measurement of the signal intensity. On the 3D-real IR image obtained at post-IV-SD-GBCA, the 3.0 mm diameter-circular ROIs were manually placed in the LV_{ante} (**a**), the LV_{tri} (**b**), the SyF (**c**), the Amb (**d**), the PPC (**e**), the CPA (**f**), and the Vit (**g**). Then, the ROIs were copied and pasted onto the 3D-real IR image obtained post-IV-SD-GBCA. 3D-real IR, 3D real inversion recovery; Amb, ambient cistern; CPA, cerebellopontine angle cistern; IV-SD-GBCA, intravenous administration of a single dose of gadolinium-based contrast agent; LV_{ante}, anterior horn of the lateral ventricle; LV_{tri}, trigone of the lateral ventricle; PPC, prepontine cistern; ROI, region of interest; SyF, Sylvian fissure; Vit, vitreous.

observed in the MR cisternography, which obtained at the same time as the 3D-real IR while the EH examination. The constant flip angle echo train readout, which was set the similar value to the MR cisternography was used in the 3D-real IR imaging. Although there might be some signal alteration due to the CSF flow, we think the effect of flow is small.[4]

Previous studies have speculated that the choroid plexus was a potential source of the leakage of intravenously administered GBCAs from blood vessels into the CSF.[11,20] This idea was based on the time course of the CSF enhancement, in which the ventricular CSF was enhanced post-IV-GBCA earlier than the enhancement of the cisternal CSF,[20] and the decrease of contrast enhancement in the choroid plexus through the LV to the third ventricle.[11] Alternatively, the characteristic finding of a strong signal enhancement in the CSF surrounding regions such as the peripheral part of the cranial nerve and the cortical veins including vein of Labbe has been reported.[10,13,14] To the best of our knowledge,

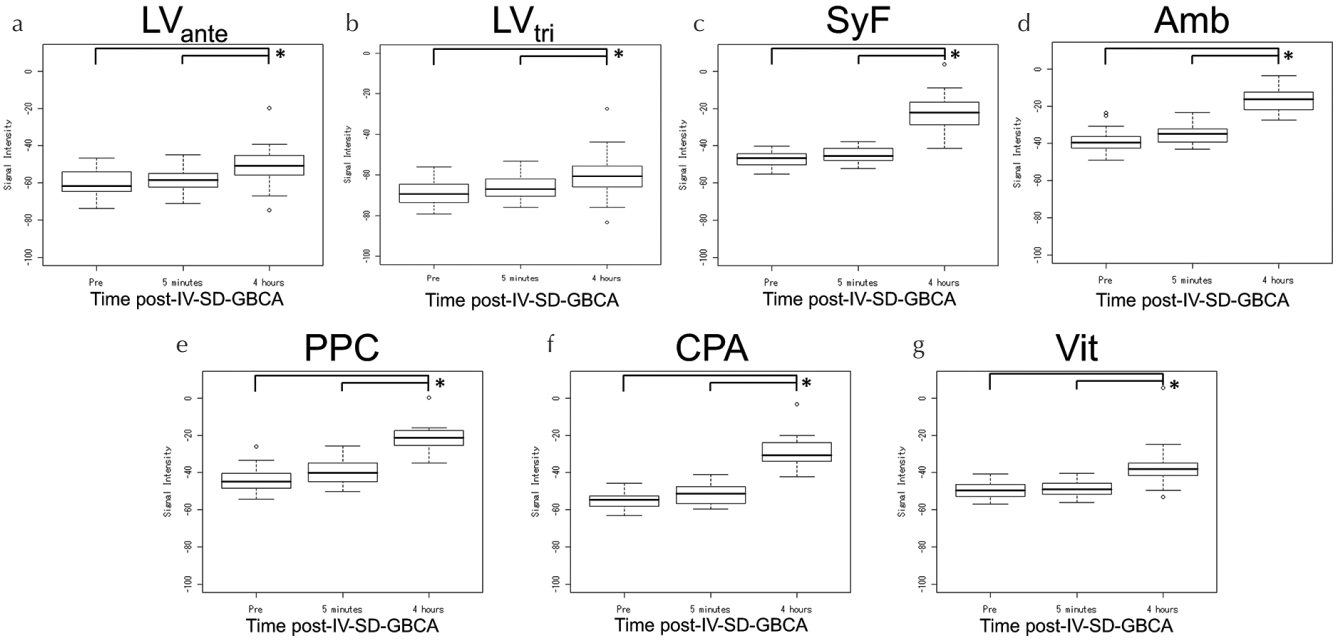

Fig. 2 A comparison of the SI between the 3D-real IR images obtained at pre-, and at 5 min, and 4 h post-IV-SD-GBCA in the LV_{ante} (**a**), the LV_{tri} (**b**), the SyF (**c**), the Amb (**d**), the PPC (**e**), the CPA (**f**), and the Vit (**g**). An asterisk (*) indicates significant differences after multiple comparisons correction ($P < 0.05$). A significant difference in the SI was observed between the 3D-real IR images obtained pre- and 4 h post-IV-SD-GBCA in all regions ($P < 0.05$). 3D-real IR, 3D real inversion recovery; Amb, ambient cistern; CPA, cerebellopontine angle cistern; IV-SD-GBCA, intravenous administration of a single dose of gadolinium-based contrast agent; LV_{ante}, anterior horn of the lateral ventricle; LV_{tri}, trigone of the lateral ventricle; PPC, prepontine cistern; SI, signal intensities; SyF, Sylvian fissure; Vit, vitreous.

Table 2 *P*-value for multiple comparison of SI

ROI location	LV_{ante}			LV_{tri}			SyF			Amb		
Time post-IV-SD-GBCA	Pre	5 min	4 h	Pre	5 min	4 h	Pre	5 min	4 h	Pre	5 min	4 h
Pre	NA			NA			NA			NA		
5 min	0.44844	NA		0.18428	NA		0.19754	NA		0.05497	NA	
4 h	0.00018*	0.00098*	NA	0.00112*	0.03424*	NA	0.00000*	0.00000*	NA	0.00000*	0.00000*	NA
ROI location	PPC			CPA			Vit					
Time post-IV-SD-GBCA	Pre	5 min	4 h	Pre	5 min	4 h	Pre	5 min	4 h			
Pre	NA			NA			NA					
5 min	0.05155	NA		0.07181	NA		0.79770	NA				
4 h	0.00000*	0.00000*	NA	0.00000*	0.00000*	NA	0.00000*	0.00001*	NA			

An asterisk (*) indicates significant difference. Amb, the ambient cistern; CPA, the cerebellopontine angle cistern; IV-SD-GBCA, intravenous administration of a single dose of gadolinium-based contrast agent; LV_{ante}, the anterior horn of the lateral ventricle; LV_{tri}, the trigone of the lateral ventricle; NA, not applicable; PPC, the prepontine cistern; ROI, region of interest; SI, signal intensity; SyF, the Sylvian fissure; Vit, the vitreous.

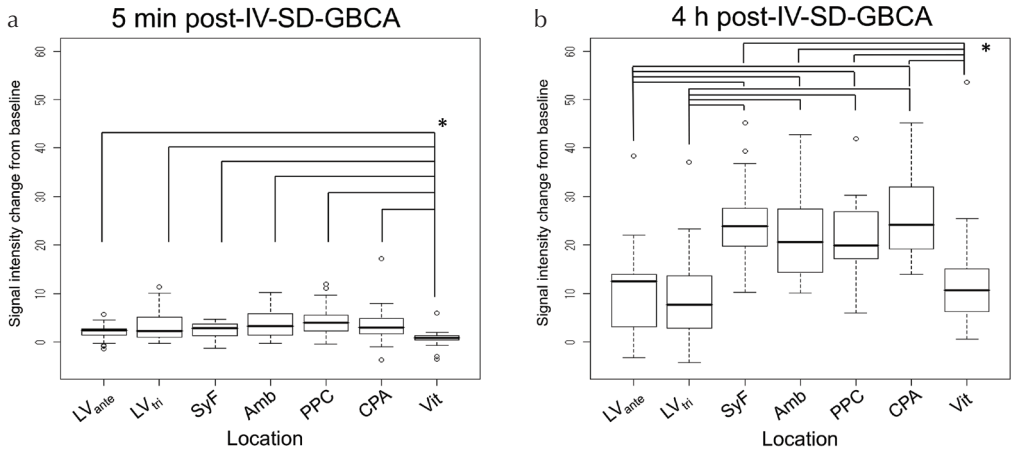

Fig. 3 A comparison of SI_{change} between the LV_{ante}, the LV_{tri}, the SyF, the Amb, the PPC, the CPA, and the Vit, on the 3D-real IR image obtained at 5 min post- (**a**) and 4 h post- (**b**) IV-SD-GBCA. The asterisk (*) indicates a significant difference after multiple comparisons correction ($P < 0.05$). A significant difference was observed between SI_{change} of the LV_{ante}, LV_{tri}, and the Vit and that of the SyF, Amb, PPC, and the CPA, in the images from 4 h post-IV-SD-GBCA ($P < 0.05$). 3D-real IR, 3D real inversion recovery; Amb, ambient cistern; CPA, cerebellopontine angle cistern; IV-SD-GBCA, intravenous administration of a single dose of gadolinium-based contrast agent; LV_{ante}, anterior horn of the lateral ventricle; LV_{tri}, trigone of the lateral ventricle; PPC, prepontine cistern; SI_{change}, the change in the signal intensity from pre-administration of contrast agent; SyF, Sylvian fissure; Vit, vitreous.

Table 3 *P*-value for multiple comparison of SI_{change}

Time post-IV-SD-GBCA	5 min							4 h						
ROI location	LV_{ante}	LV_{tri}	SyF	Amb	PPC	CPA	Vit	LV_{ante}	LV_{tri}	SyF	Amb	PPC	CPA	Vit
LV_{ante}	NA							NA						
LV_{tri}	0.92329	NA						0.99768	NA					
SyF	0.90495	0.99289	NA					0.00001*	0.00001*	NA				
Amb	0.45343	0.99841	0.69917	NA				0.00024*	0.00007*	0.89836	NA			
PPC	0.05867	0.94396	0.27781	0.99975	NA			0.00007*	0.00005*	0.85253	1.00000	NA		
CPA	0.26809	0.99958	0.89142	1.00000	0.98261	NA		0.00000*	0.00000*	1.00000	0.73349	0.71077	NA	
Vit	0.01513*	0.00617*	0.00804*	0.00471*	0.00076*	0.00383*	NA	0.89836	0.89836	0.00005*	0.00082*	0.00103*	0.00004*	NA

An asterisk (*) indicates significant difference. Amb, the ambient cistern; CPA, the cerebellopontine angle cistern; IV-SD-GBCA, intravenous administration of a single dose of gadolinium-based contrast agent; LV_{ante}, the anterior horn of the lateral ventricle; LV_{tri}, the trigone of the lateral ventricle; NA, not applicable; PPC, the prepontine cistern; ROI, region of interest; SI_{change}, the change in the signal intensity from pre-administration of contrast agent; SyF, the Sylvian fissure; Vit, the vitreous.

there are no reports showing such distinct contrast enhancement in the lateral ventricular CSF surrounding the choroid plexus, including our patients' images. A previous study of CSF dynamics proposed a new hypothesis that CSF secretion and absorption occurs everywhere in the brain, and the choroid plexus could be considered as only one part of the circulation system.[21] In addition, this present study showed a higher concentration of intravenously administered GBCAs in the cisternal CSF than in the lateral ventricular CSF. The ventricular CSF volume is larger than that of the cisterns, which may result in more diluted GBCA within that region. However, we confirmed that there was no difference in CSF enhancement between the LV_{ante} and the LV_{tri}. Therefore, the choroid plexus might be just "one site" where the GBCA from the blood vessels leaks into the CSF, and not the main pathway of such leakage. The CSF plays an important role in clearance of the waste in the brain through the glymphatic pathway.[7] Accumulation of the interstitial solutes in the brain due to the glymphatic dysfunction causes the neurodegenerative change such as Alzheimer's disease.[7] The CSF homeostasis would be closely related to the regulation of glymphatic system. In this present study, we confirmed the difference in the distribution of intravenously administrated GBCA depending on the location of CSF in the brain. Age-related leakage of GBCA in the CSF surrounding the cortical veins has been suggested.[13] As a further study, the relationship

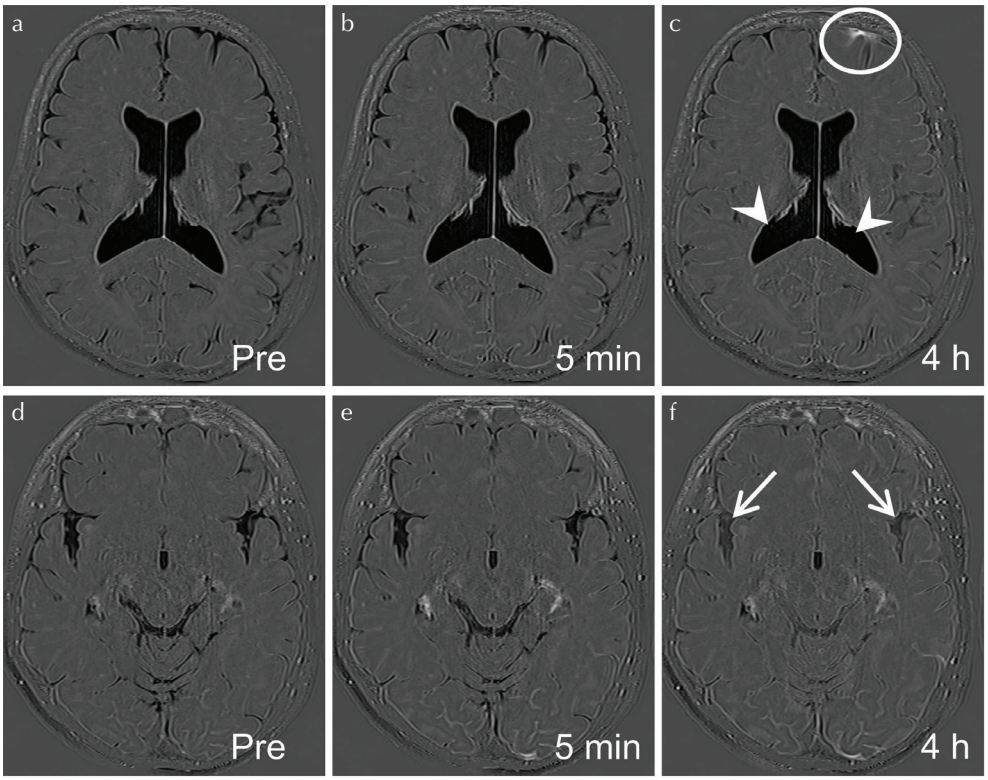

Fig. 4 A 57-year-old woman with clinically suspected endolymphatic hydrops. The 3D-real IR images obtained pre- (**a**), 5 min post- (**b**), and 4 h post- (**c**) IV-SD-GBCA at the lateral ventricular level, and pre- (**d**), 5 min post- (**e**), and 4 h post- (**f**) IV-SD-GBCA at the SyF level. The contrast enhancement of the CSF is shown in the image obtained at 4 h post-IV-SD-GBCA (**c**) and (**f**), and the degree of the enhancement in the SyF (**f**, arrows) was greater than that in the lateral ventricle (**c**, arrow heads). The strong CSF enhancement, which indicates leakage of the GBCA was observed in the superficial subarachnoid space (**c**, circle). 3D-real IR, 3D real inversion recovery; CSF, cerebrospinal fluid; IV-SD-GBCA, intravenous administration of a single dose of gadolinium-based contrast agent; SyF, Sylvian fissure.

between GBCA distribution and aging would be interesting for elucidating behavior of fluid in the central neural system.

The enhancement in the vitreous after IV-GBCA was also evaluated in this study, because the vitreous, which is mainly composed of fluid, was included within the imaging field of view. In one patient with a clinical history of cataract lens replacement, a strong enhancement at post-IV-SD-GBCA was observed. However, we considered this to be an outlier. The leakage of intravenously administered GBCA into the ocular structure including the vitreous has been reported in patients with a disruption of the blood-ocular barrier such as in acute cerebral stroke.[22] However, other patients in this current study also showed the GBCA distribution in the vitreous after IV-SD-GBCA as in the previous report.[11] Recently, impaired CSF circulation causing toxic fluid environment in the subarachnoid space surrounding the optic nerve has been suggested as one of the causes of glaucoma with normal intraocular pressure.[23] The CSF surrounding the subarachnoid space of the optic nerve is reported one part where intravenously administered GBCA leaks.[10] The GBCA permeability of the blood–ocular barrier might be related to the cause of the ocular disease.

This study includes some limitations. First, there was a small number of subjects. Second, all subjects were patients with a suspicion of EH with bolus IV-GBCA. An investigation with a larger number of healthy subjects would be valuable to further establish these findings under normal conditions. Slow continuous IV-GBCA might be valuable to rule out the possibility of intermittent leakage of GBCA from choroid plexus. Third, the ROIs were placed manually. As a result, the measurements between the two observers were comparable in this study. However, a bias free automatic volume segmentation would be warranted as a further study.

Conclusion

The GBCA concentration was higher in the cisterns than in the LVs 4 h post-IV-SD-GBCA. The choroid plexus may not be the main pathway by which intravenously administered GBCA leaks into the CSF.

Conflicts of Interest

None of the authors have any conflicts of interest regarding this study.

References

1. Kanda T, Ishii K, Kawaguchi H, Kitajima K, Takenaka D. High signal intensity in the dentate nucleus and globus pallidus on unenhanced T_1-weighted MR images: relationship with increasing cumulative dose of a gadolinium-based contrast material. Radiology 2014; 270:834–841.
2. Naganawa S, Kawai H, Sone M, Nakashima T. Increased sensitivity to low concentration gadolinium contrast by optimized heavily T_2-weighted 3D-FLAIR to visualize endolymphatic space. Magn Reson Med Sci 2010; 9:73–80.
3. Kato Y, Bokura K, Taoka T, Naganawa S. Increased signal intensity of low-concentration gadolinium contrast agent

by longer repetition time in heavily T_2-weighted-3D-FLAIR. Jpn J Radiol 2019; 37:431–435.
4. Naganawa S, Nakane T, Kawai H, Taoka T. Gd-based contrast enhancement of the perivascular spaces in the basal ganglia. Magn Reson Med Sci 2017; 16:61–65.
5. Rasschaert M, Schroeder JA, Wu TD, et al. Multimodal imaging study of gadolinium presence in rat cerebellum: differences between Gd chelates, presence in the Virchow-Robin space, association with lipofuscin, and hypotheses about distribution pathway. Invest Radiol 2018; 53:518–528.
6. Taoka T, Jost G, Frenzel T, Naganawa S, Pietsch H. Impact of the glymphatic system on the kinetic and distribution of gadodiamide in the rat brain: observations by dynamic MRI and effect of circadian rhythm on tissue gadolinium concentrations. Invest Radiol 2018; 53:529–534.
7. Iliff JJ, Wang M, Liao Y, et al. A perivascular pathway facilitates CSF flow through the brain parenchyma and the clearance of interstitial solutes, including amyloid β. Sci Transl Med 2012; 4:147ra111.
8. Taoka T, Naganawa S. Gadolinium-based contrast media, cerebrospinal fluid and the glymphatic system: possible mechanisms for the deposition of gadolinium in the brain. Magn Reson Med Sci 2018; 17:111–119.
9. Taoka T, Naganawa S. Glymphatic imaging using MRI. J Magn Reson Imaging 2020; 51:11–24.
10. Naganawa S, Suzuki K, Yamazaki M, Sakurai Y. Serial scans in healthy volunteers following intravenous administration of gadoteridol: time course of contrast enhancement in various cranial fluid spaces. Magn Reson Med Sci 2014; 13:7–13.
11. Deike-Hofmann K, Reuter J, Haase R, et al. Glymphatic pathway of gadolinium-based contrast agents through the brain: overlooked and misinterpreted. Invest Radiol 2019; 54:229–237.
12. Naganawa S, Taoka T, Kawai H, Yamazaki M, Suzuki K. Appearance of the organum vasculosum of the lamina terminalis on contrast-enhanced MR imaging. Magn Reson Med Sci 2018; 17:132–137.
13. Naganawa S, Nakane T, Kawai H, Taoka T. Age dependence of gadolinium leakage from the cortical veins into the cerebrospinal fluid assessed with whole brain 3D-real inversion recovery MR imaging. Magn Reson Med Sci 2019; 18:163–169.
14. Ohashi T, Naganawa S, Ogawa E, Katagiri T, Kuno K. Signal intensity of the cerebrospinal fluid after intravenous administration of gadolinium-based contrast agents: strong contrast enhancement around the vein of Labbe. Magn Reson Med Sci 2019; 18:194–199.
15. Naganawa S, Yamazaki M, Kawai H, Bokura K, Sone M, Nakashima T. Imaging of Ménière's disease after intravenous administration of single-dose gadodiamide: utility of subtraction images with different inversion time. Magn Reson Med Sci 2012; 11:213–219.
16. Naganawa S, Ohashi T, Kanou M, Kuno K, Sone M, Ikeda M. Volume quantification of endolymph after intravenous administration of a single dose of gadolinium contrast agent: comparison of 18- versus 8-minute imaging protocols. Magn Reson Med Sci 2015; 14:257–262.
17. Naganawa S, Kawai H, Taoka T, Sone M. Improved 3D-real inversion recovery: a robust imaging technique for endolymphatic hydrops after intravenous administration of gadolinium. Magn Reson Med Sci 2019; 18:105–108.
18. Ohashi T, Naganawa S, Takeuchi A, Katagiri T, Kuno K. Quantification of endolymphatic space volume after intravenous administration of a single dose of gadolinium-based contrast agent: 3D-real inversion recovery versus HYDROPS-Mi2. Magn Reson Med Sci 2019; 19:119–124.
19. Fukuoka H, Hirai T, Okuda T, et al. Comparison of the added value of contrast-enhanced 3D fluid-attenuated inversion recovery and magnetization-prepared rapid acquisition of gradient echo sequences in relation to conventional postcontrast T_1-weighted images for the evaluation of leptomeningeal diseases at 3T. AJNR Am J Neuroradiol 2010; 31:868–873.
20. Jost G, Frenzel T, Lohrke J, Lenhard DC, Naganawa S, Pietsch H. Penetration and distribution of gadolinium-based contrast agents into the cerebrospinal fluid in healthy rats: a potential pathway of entry into the brain tissue. Eur Radiol 2017; 27:2877–2885.
21. Orešković D, Radoš M, Klarica M. Role of choroid plexus in cerebrospinal fluid hydrodynamics. Neuroscience 2017; 354:69–87.
22. Hitomi E, Simpkins AN, Luby M, Latour LL, Leigh RJ, Leigh R. Blood-ocular barrier disruption in patients with acute stroke. Neurology 2018; 90:e915–e923.
23. Killer HE, Pircher A. Normal tension glaucoma: review of current understanding and mechanisms of the pathogenesis. Eye (Lond) 2018; 32:924–930.